Available online at www.sciencedirect.com

ScienceDirect

Physics Procedia 56 (2014) 228 – 238

Physics Procedia

8th International Conference on Photonic Technologies LANE 2014

Correlations of melt pool geometry and process parameters during laser metal deposition by coaxial process monitoring

Sörn Ocylok[a]*, Eugen Alexeev[a], Stefan Mann[a], Andreas Weisheit[a], Konrad Wissenbach[a], Ingomar Kelbassa[b]

[a]*Fraunhofer Institute for Laser Technology Steinbachstraße 15, 52074 Aachen, Germany*
[b]*RWTH Aachen University, Chair for Laser Technology Steinbachstraße 15, 52074 Aachen, Germany*

Abstract

One major demand of today's laser metal deposition (LMD) processes is to achieve a fail-save build-up regarding changing conditions like heat accumulations. Especially for the repair of thin parts like turbine blades is the knowledge about the correlations between melt pool behavior and process parameters like laser power, feed rate and powder mass stream indispensable. The paper will show the process layout with the camera based coaxial monitoring system and the quantitative influence of the process parameters on the melt pool geometry. Therefore the diameter, length and area of the melt pool are measured by a video analytic system at various parameters and compared with the track wide in cross-sections and the laser spot diameter. The influence of changing process conditions on the melt pool is also investigated. On the base of these results an enhanced process of the build-up of a multilayer one track fillet geometry will be presented.

Peer-review under responsibility of the Bayerisches Laserzentrum GmbH

Keywords: process monitoring; laser metal deposition

1. Introduction

Due to the demand of increasing the quality of parts built by laser metal deposition knowledge of correlations between the main process parameters laser power, feed rate, powder mass stream and the melt pool behavior is

* Corresponding author. Tel.: +49-241-890-6567; fax: +49-241-890-6121.
E-mail address: soern.ocylok@ilt.fraunhofer.de

Peer-review under responsibility of the Bayerisches Laserzentrum GmbH
doi:10.1016/j.phpro.2014.08.167

required. Especially for the further development of a process control regarding the installation of a fully automated LMD process these fundamental dependencies are indispensable. Schmidt observed that a pyrometric system with only one wavelength is not suitable for the LMD process, cause of its dependence of the material emissivity (Schmidt 1993). The additional control of the layer thickness by a CCD-camera based system was investigated by Toyserkani et al. 2004. In the recent past different process monitoring systems with pyrometric or camera-based devices were investigated (Hu et al. 2003) and compared (Colodrón et al. 2011). The temperature distribution in the melt pool is hardly affected by the used intensity distribution of the laser radiation e.g. a top-hat-distribution has a lower maximum temperature in the middle of the melt pool in comparison to a gauss-profile by using the same parameters (Bi et al. 2013). The melt pool geometry and its temperature have a large effect on the track geometry and the process result, but today´s process control systems are on development stage (Hofman et al. 2012). Certain control systems were developed to improve the process stability, especially for the build-up of thin structures (Jiang et al.2006; Nan et al. 2006). Also the influence of process parameters on the dilution rate was investigated (Hofman et al. 2011). The temperature distribution in the melt pool depends on process parameters but also on the used intensity profile of the laser radiation (Smurov et al. 2012). One main disadvantage in many past investigations is the use of a monochromatic pyrometer and its need of an adjustment to a certain emission degree, which hardly depends on the material behavior and the temperature. Camera-based systems must in contrast to pyrometric devices not be adjusted to a material or temperature. The measurement of the exact temperature is even with two-colour pyrometers challenging caused of the need of an installation under a constant angle, which was already shown by Bi et al. 2006. In comparison to the state-of-art the achieved results will give a comprehensive analysis of the influences of the main process parameters (laser power, feed rate and powder mass stream) on the melt pool geometry. The main aim of the experiments is to determinate the correlations between melt pool geometry and process parameters in a wide range for generating an improved knowledge about the laser metal deposition process.

2. Laser metal deposition process

Laser metal deposition (LMD) is a powder-based process to build up 3D parts layer by layer (Gasser et al. 2003). The powder can be fed either off-axially or coaxially. Figure 1 shows a continuous coaxial powder feed nozzle used for the experiments. The powder is fed by an inert gas stream (e.g. helium or argon) to the treatment area, where it is melt by the laser radiation. After solidification a layer with a metallurgical bonding to the substrate is produced. By adaptation of the process parameters such as velocity, powder feed rate and laser power, the thickness of the built layer can be varied typically from 0.1 up to 3 mm in a single pass. With multi-layer cladding thicker layers can be produced. The main advantages of the laser cladding process are high precision, a minimized heat affected zone (HAZ), low distortion and the variety of materials. Nearly every metallic material can be cladded. Low melting alloys based on aluminium can be used as well as nickel-based alloys, intermetallics (e.g. titanium aluminide) and high-melting point metals such as tungsten.

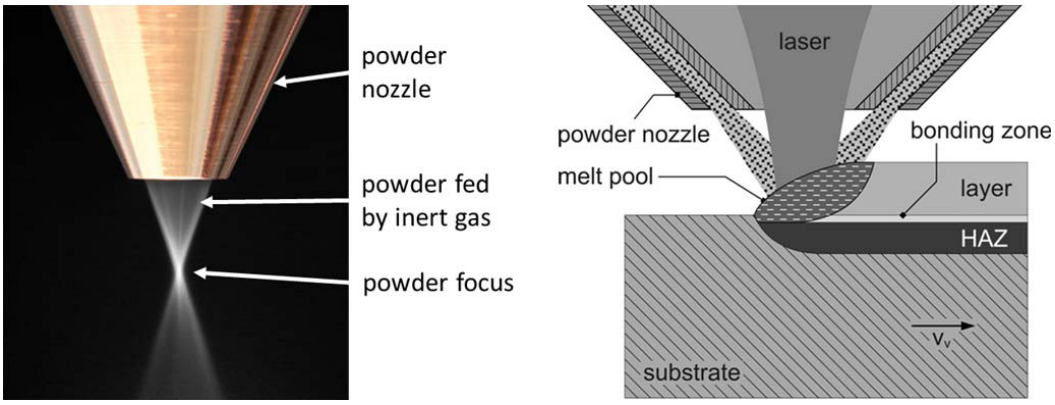

Fig. 1. (a) Continuous coaxial powder nozzle; (b) Schematic LMD process.

The powder is fed to the interaction zone in a carrier gas stream (helium or argon). The laser beam melts the powder material particles and a thin layer of the base material (Figure 1b). This method is also used for the production of graded layers.

3. Equipment and materials

For carrying out the experimental investigations a numeric controlled 5-axis handling system with a 3kW fibre-coupled diode laser with a 976nm wavelength is used. After the collimation optics the laser radiation is reflected at a dichroitic mirror into the focal optic system (Fig. 2). The laser spot has a focus diameter of 1.7 mm which is adjusted to the surface of the base material, where also the powder material is fed coaxially by the nozzle to the treatment area. The intensity distribution at different laser power ratings was analyzed by with a Primes Focus Monitor. The back reflection of the melt pool passes a colored filter and the optic system before it is recorded by the CMOS-camera (Fig. 2).
As base material the hot working tool steel X38CrMoV 5-1 is used. For the powder formed addition material (particle distribution of 45-100µm) the tool steel 32CrMoV 12-28 is chosen, cause of the use for many tooling applications and its wide applicable process parameter window.

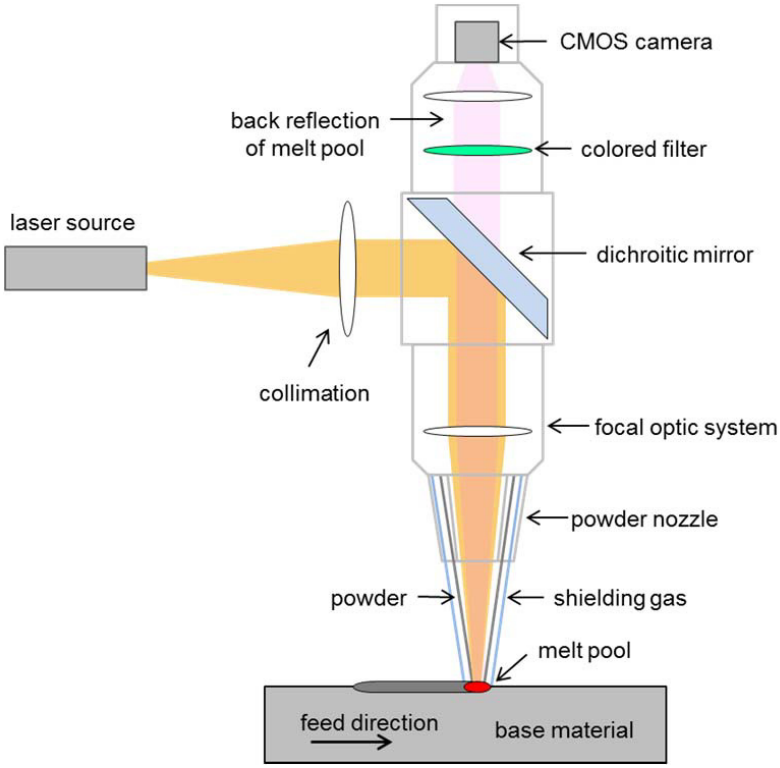

Fig. 2. Schematic diagram of CPC-System

4. Processing

For the experimental investigations of the melt pool geometry single tracks with different combinations of the process parameters (table 1) were built up. The length of the tracks (40 – 80 mm) was adapted to the feed rate to achieve a comparable number of images.

Table 1. Investigated process parameters

Process Parameter	Min. Value	Max. Value
Laser power [W]	600	1800
Feed rate [mm/min]	300	1200
Powder mass stream [g/min]	1.2	4.8

In the first step video grapping software must be adjusted regarding the contrast at various process parameters for the later measuring of the melt pool. Therefore a set of parameters (expose time, frame rate, solution) which is suitable for low and high energy intensities is found.
In the second step a threshold is set for the calculation of a frame which surrounds the melt pool for the later measuring of its geometry. The threshold has a large influence on the binarisation step, which is necessary for the automated measuring of the melt pool size. Small threshold values increase the measured size by enlarging the measuring frame in the binarised image (Fig. 3b). The threshold is set to a value, where the frame fits exactly to the bright area of the melt pool (Fig. 3c). The calculated frame is adapted automatically by the analysis software for every single image so the width, length and area size of the melt pool is measured for each image.

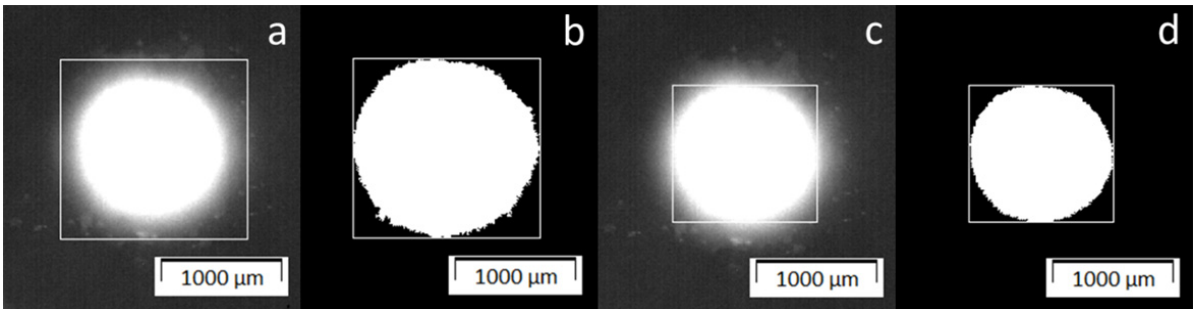

Fig. 3. Image of melt pool (a) threshold too small; (b) second picture (c) threshold too small; (d) second picture..

In comparison to the width of the single tracks, which are measured in cross sections, a nearly constant deviation of 150 µm to the measured melt pool width was detected. This enlargement of the track width is caused by heat conductivity and the viscosity of the melt.
Beside the enlargement of the track width sparks have a huge influence on the measuring of the melt pool width and length (Fig. 4). The increase of the measured melt pool width and length by these disturbances is less than 0.5%. The number of sparks is between 10 and 20 per single track with a length of 40 mm

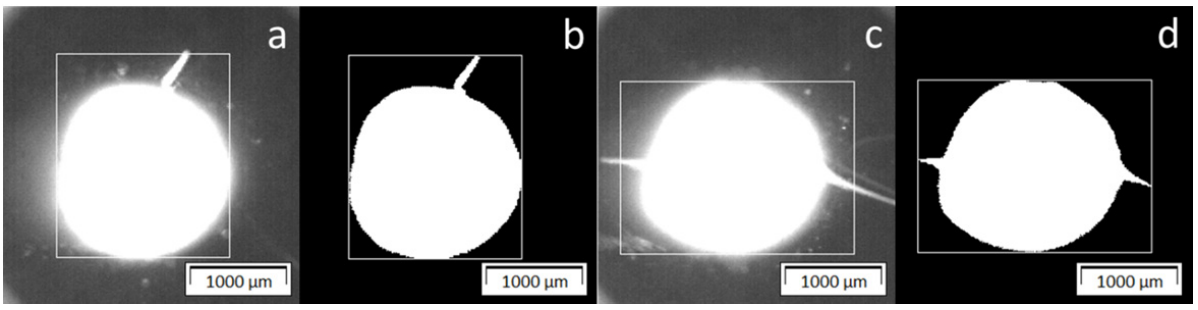

Fig. 4. Disturbances during measuring by sparks (a) width of melt pool; (b) length of melt pool.

The recorded data of the melt pool geometry during the built up of a single track (Fig. 5) shows, that the melt pool length is larger than the width, which is caused by the direction of feed motion. In comparison to the linear value of

length and width the melt pool area size is less affected by disturbances e.g. sparks. Therefore in the following results the melt pool size is chosen for analysing the influence of the process parameters.

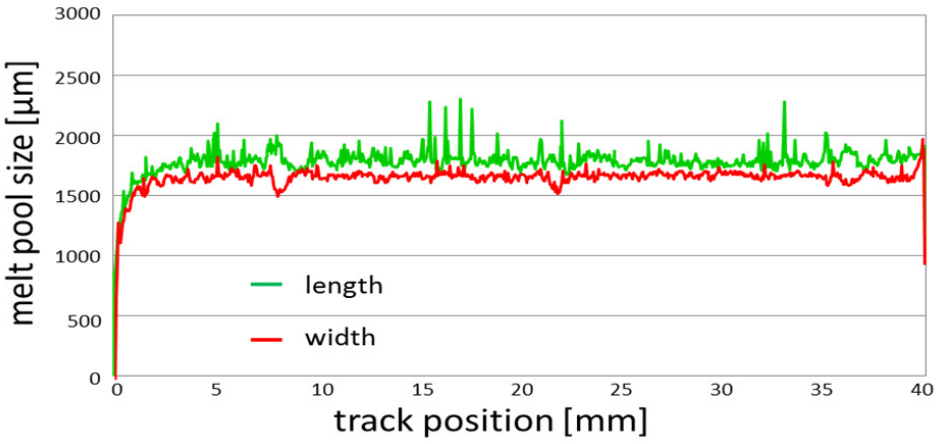

Fig. 5. Recorded melt pool size of a single track (900 W, 600 mm/min, 2,45 g/min)

In the following the measured melt pool sizes are values averaged by more than 500 images. The average size was calculated excluding the first tenth of a second, where the melt pool is created on the substrate. Also the enlargement of the melt pool at the end of the track, where the handling system slows down before reaching the end position is not considered in the calculation.

5. Results

The increase of the spot diameter adds up to 30µm (from 1744 to 1774 µm) for a triplication of the laser power from 600 to 1800 W. In comparison to the investigated process parameters the influence of the laser power on the spot diameter is negligible. The enlargement of the melt pool geometry by an increase of the laser power from 700 W to 1200 W is significant (Fig. 6 a-c). The further process parameters of the feed rate (600 mm/min) and powder mass flow (2.45 g/min) were kept constant for investigation on the influence of the laser power.

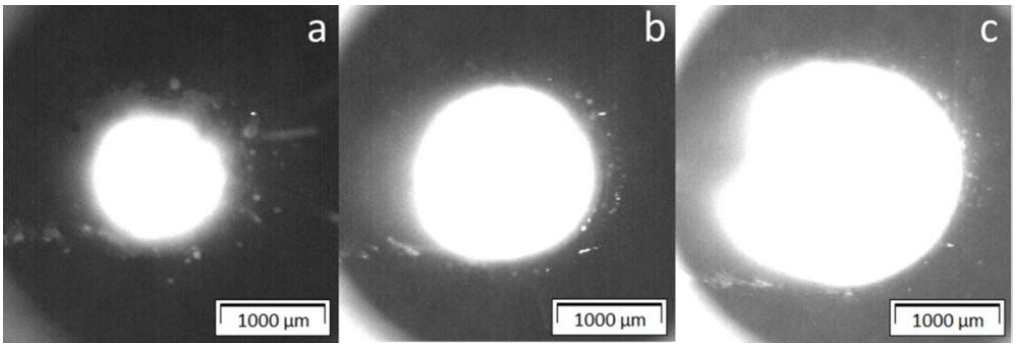

Fig. 6. Variation of laser power (a) 700 W; (b) 900 W; (c) 1200 W.

At a laser power of less than 900 W the intensity of the laser radiation is too small to create a melt pool with the size of the spot diameter, which is nearly constant at 2.4 mm^2 for the investigated laser power values. The enlargement of the melt pool size by an increase of the laser power is almost linear. These results demonstrate that the achieved width of a single track depends not only on the spot diameter. The laser power has a major influence on the melt

pool size (Fig. 7).

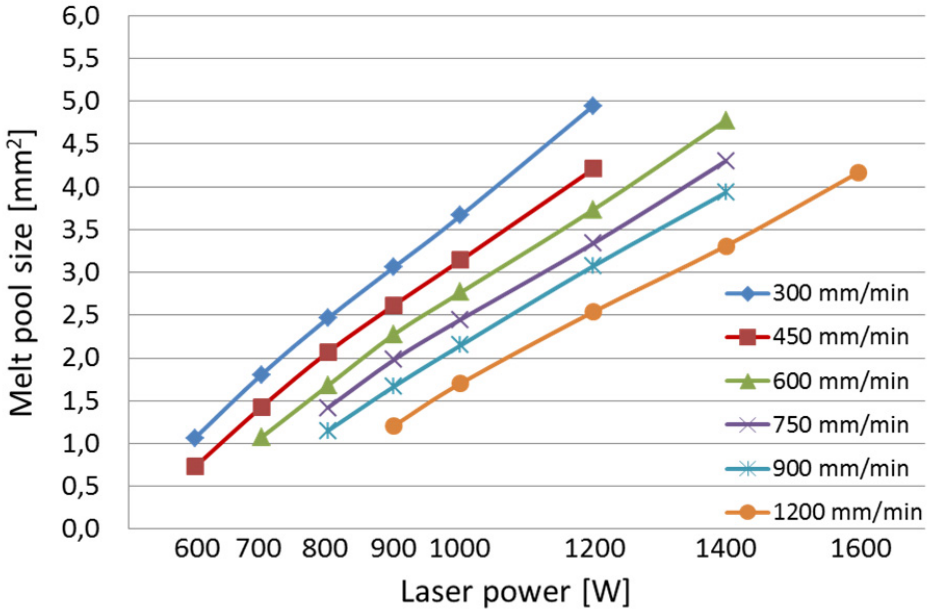

Fig. 7. Melt pool size in dependence of laser power and feed rate

An increase of the laser power also increases the energy input per unit length. For an efficient process the knowledge about the required energy for building up a track with a certain width is essential. At low feed rates the energy input for building up a single track with a certain width is much higher in comparison to higher feed rates (Fig. 8). At low feed rates the loss of the energy by heat conductivity is much higher in comparison to higher feed rates, which results in a larger heating of the surrounding substrate material.

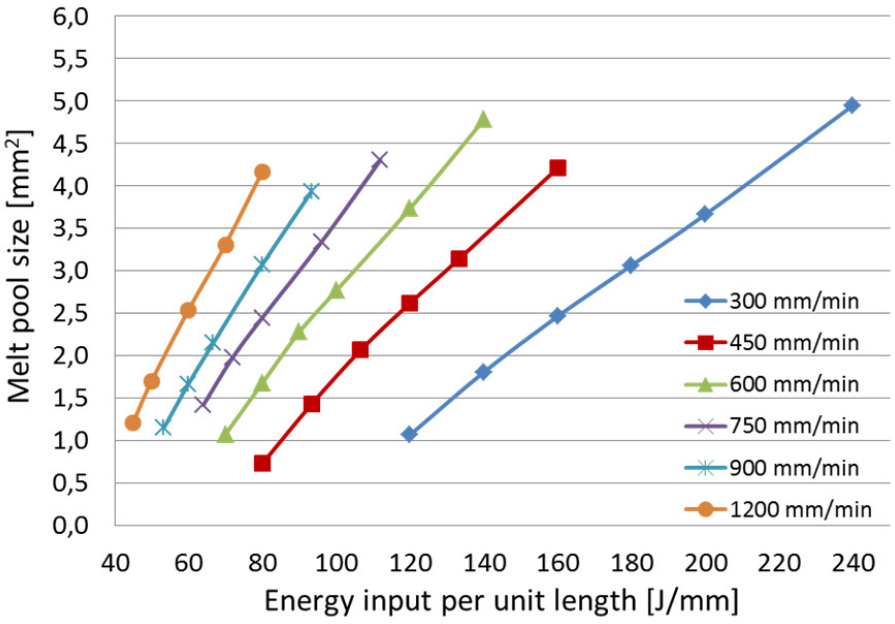

Fig. 8. Melt pool size in dependence of energy input

The correlation between feed rate and melt pool size is negative, so an increase of the feed rate decreases the melt pool size (Fig. 8).

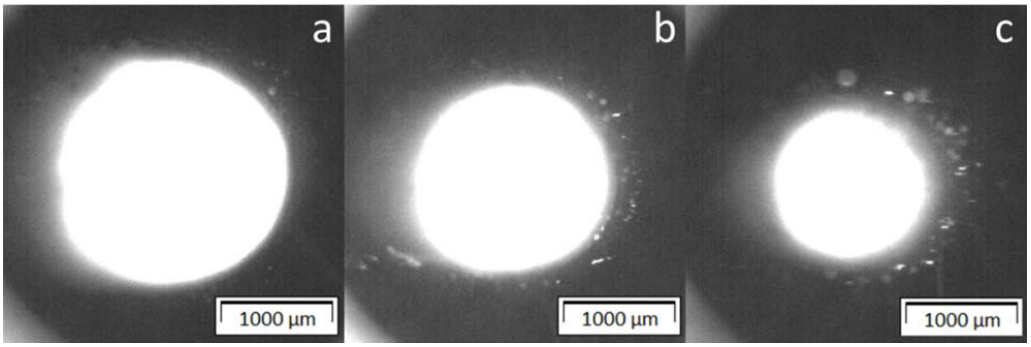

Fig. 9. Variation of feed rate (a) 300 mm/min; (b) 600 mm/min; (c) 1200 mm/min.

The influence of the feed rate on the melt pool size is much smaller in comparison to the influence of the laser power. A decrease of the feed rate from 600 mm/min to 300 mm/min doubles the energy input and leads to an enlargement of the melt pool from 2.28 mm^2 (Fig. 9b) to 3.06 mm^2 (Fig. 9a), which is an increase of 34.2 %. In comparison leads a doubled energy input by an increase of the laser power from 700 W up to 1400 W at a constant feed rate of 600 mm/min to an enlargement of the melt pool from 1.072 mm^2 to 4.778 mm^2, which is an increase of 346 %.

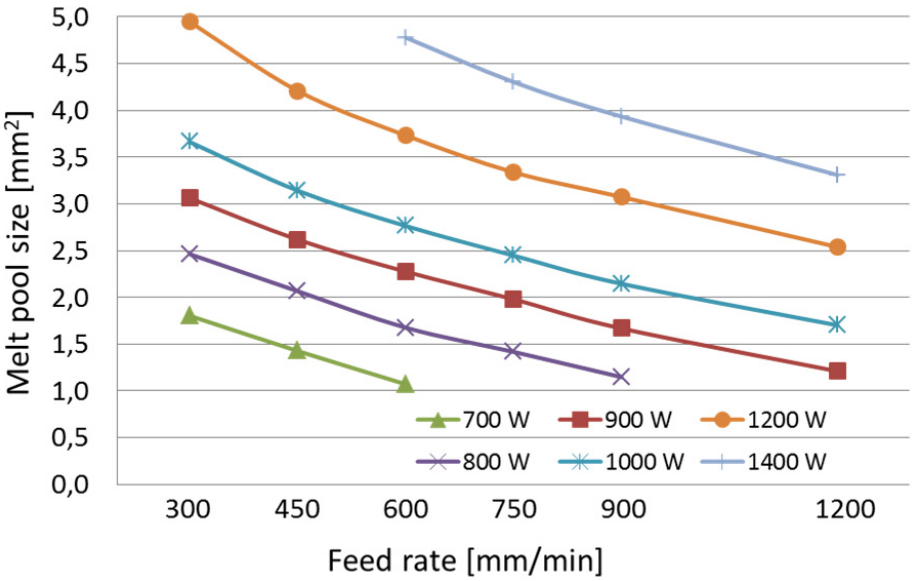

Fig. 10. Variation of feed rate (a) 300 mm/min; (b) 600 mm/min; (c) 1200 mm/min.

The powder mass flow has the smallest influence on the melt pool size of the three investigated process parameters. A four times larger powder mass flow form 1.2 g/min up to 4.8 g/min leads to a small decrease of the melt pool size from 2.28 mm^2 to 2.08 mm^2 (Fig. 11a, b). This negative correlation can be explained by the higher required energy input, which is necessary to melt the additional powder material, so less energy is left to heat up the base material in the treatment area to create a melt pool. By increasing the powder mass flow the thickness of the single track increases nearly linear and the depth of penetration in the base material decreases continuously.

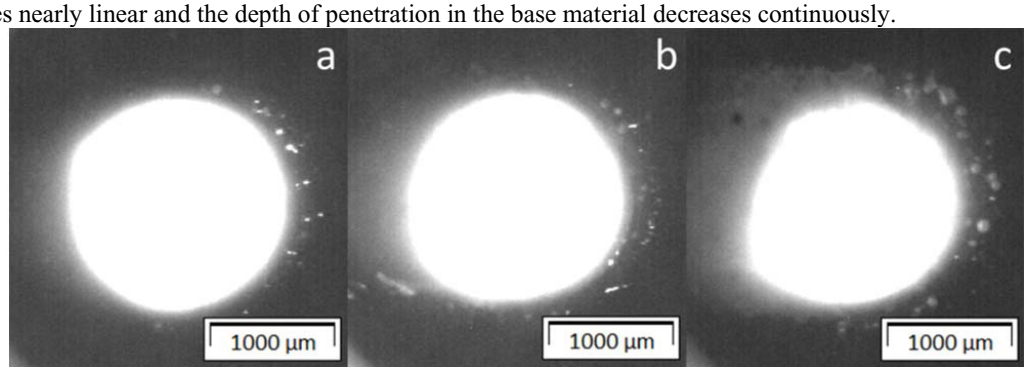

Fig. 11. Variation of powder mass flow (a) 1.2 g/min; (b) 2.4 g/min; (c) 4.8 g/min.

Beside the influence of the three investigated process parameters the heating of the base material during a built up process also influences the melt pool size. A preheating up to 300°C increases the melt pool size in comparison to room temperature by more than 20% at all investigated laser power values.

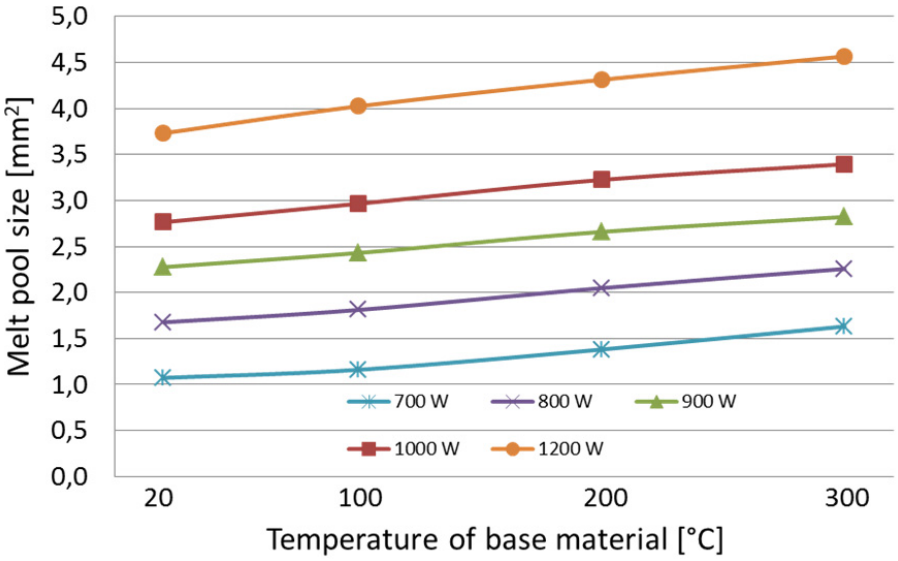

Fig. 12. Melt pool size in dependence of base material temperature.

After determination of the correlations between the investigated process parameters a single track multilayer fillet was built up with a constant laser power of 800 W, a feed rate of 600 mm/min and a powder mass flow of 2.45 g/min. The melt pool size was measured for each layer (Fig. 13). On the base of the results of the variation of the laser power at a feed rate of 600 mm/min the adapted laser power values were calculated for each layer (table 2).

Table 2. Adapted laser power for fillet buildup

Number of layer	1	2	3	4	5	6-15
Laser power [W]	940	900	875	850	825	800
Feed rate [mm/min]	600					
Powder mass stream [g/min]	2.45					

The melt pool size during the build-up with the adapted laser power is nearly constant after the third layer. The smaller melt pool area in the first two layers is caused by the higher heat conductivity to the base material.

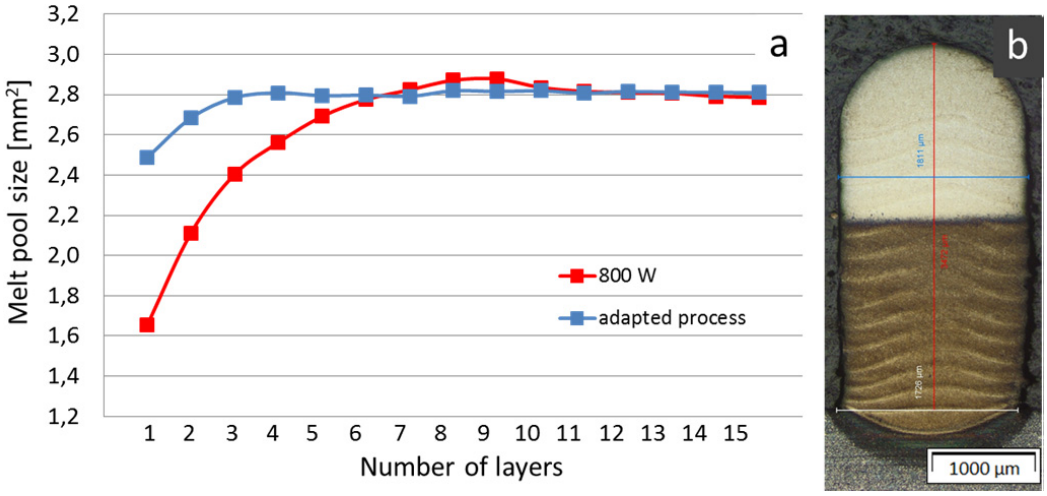

Fig. 13. (a) Melt pool size during buildup of multilayer fillet; (b) cross section of fillet

6. Conclusions

The analysis of the recorded melt pool geometry shows that in comparison to the width and length of the melt pool its size is less disturbed by sparks and other inconstancies during the LMD process. The results of the experimental investigations show the influence of the main process parameters of the LMD process (laser power, feed rate, powder mass flow) on the melt pool size. The laser power has a positive correlation to the melt pool size and the largest influence in comparison to the other process parameters. The increase of the melt pool size is nearly linear to the used laser power. An enlargement of the melt pool at constant energy inputs was also detected for an increase of the feed rate. The powder mass flow is strongly correlated to the achieved track thickness but it did not affect the melt pool size significantly. Furthermore the melt pool increases by a preheating of the base material, which is important for generating of complete parts or thin structures, where a heating up during the LMD process is observed.

The demand of correcting variable can be fulfilled by the laser power parameter, which is suitable for a quick adaptation in a process control system. The feed rate and the powder mass flow are not capable of adapting the melt pool size without influencing the thickness of the track or layer.

Finally a potential of a process control is demonstrated at the buildup of a thin one track multilayer fillet by an adaptation of the laser power in dependence of the number of layers.

References

Asselin, M.; Toyserkani, E.; Iravani-Tabrizipour, M.; Khajepour, A. (2005). Development of Trinocular CCD-Based Optical Detector for Real-Time Monitoring of Laser Cladding. International Conference on Mechatronics & Automation (P. 1190 – 1196)

Bi, G., Gasser, A., Wissenbach, K., Drenker, A., Poprawe, R. (2006). Characterization of the process control for the direct laser metallic powder deposition. Surface & Coatings Technology (201, P.2676–2683).

Bi, G., Gasser, A., Wissenbach, K., Drenker, A., Poprawe, R. (2006). Identification and qualification of temperature signal for monitoring and control in laser cladding. Optics and Lasers in Engineering(44, P.1348–1359).

Bi, G., Sun, C., Gasser, A. (2013). Study on influential factors for process monitoring and control in laser aided additive manufacturing. Journal of Materials Processing Technology(213 P. 463 – 468).

Colodrón, P., Fariña, J., Rodríguez-Andina, J. J., Vidal, F., Mato, J. L., Montealegre, Á. (2011). FPGA-Based Measurement of Melt Pool Size in Laser Cladding Systems. Vigo, Spain; Porriño, Spain.

Colodrón, P., Fariña, J., Rodríguez-Andina, J. J., Vidal, F., Mato, J. L., Montealegre, Á. (2011). Performance Improvement of a Laser Cladding System through FPGA-based Control. IEEE. (P. 2814 – 2819)

Doubenskaia, M.; Bertrand, P.; Smurov, I. (2004). Optical monitoring of Nd:YAG laser cladding. Thin Solid Films (P. 477 – 485)

Gasser, A. and Wissenbach, K. (2003). Laserstrahl-Auftragschweißen im Werkzeug- und Formenbau, Forschungsgemeinschaft Werkzeuge und Werkstoffe , 13. Werkzeugseminar

Hofman, J., Pathiraj, B., van Dijk, J., de Lange, D., Meijer, J. (2012). A camera based feedback control strategy for the laser cladding process. Journal of Materials Processing Technology (212, P. 2455 – 2462).

Hofman, J.; de lange, D.; Pathiraj, B.; Meijer, J. (2011). FEM modeling and experimental verification for dilution control in laser cladding. Journal of Materials Processing Technology 211(P. 187 – 196)

Hu, D., Kovacevic, R. (2003). Sensing, modeling and control for laser-based additive manufacturing. International Journal of Machine Tools and Manufacture(43, P.51–60).

Jiang, S.; Liu, W.; Xing, F. (2006). Research on Measuring and Control System of Metal Powder Laser Shaping. Proceedings of the 6th World Congress on Intelligent Control and Automation (P. 1717 – 1721)

Meriaudeau, F.; Truchetet, F.; Grevey, D.; Vannes, A.B. (1997). Laser cladding process and image processing. Journal of Lasers in Engineering, Vol. 6 (P. 161 – 187)

Nan, L.; Liu, W. (2006). Sensing and Control for Geometry Stability of the Melt Pool and the Cross Sectional Area in Laser Cladding. International Conference on Innovative Computing, Information and Control

Schmidt., A. (1993). Untersuchung der Wärmestrahlung laserinduzierter Schmelzbäder, Master thesis. RWTH Aachen.

Song, L. (2011). Feedback control of melt pool temperature during laser cladding process. IEEE Transactions on control systems technology, Vol. 19, No. 6 (P. 1349 – 1356)

Smurov, I.; Doubenskaia, M.; Zaitsev, A. (2012). Complex analysis of laser cladding based on comprehensive optical diagnostics and numerical simulation. Physics Procedia 39 (P. 743 – 752)

Toyserkani, E. K. (2004). Laser Cladding. CRC Press.

Xing, F.; Liu, W.; Wang, T. (2006). Real-time Sensing and Control of Metal Powder Laser Forming. Proceedings of the 6th World Congress on Intelligent Control and Automation (P. 6661 – 6665)